

# Ocular Developmental Abnormalities and Glaucoma Associated with Interstitial 6p25 Duplications and Deletions

Ordan J. Lehmann,<sup>1</sup> Neil D. Ebenezer,<sup>1</sup> Rosemary Ekong,<sup>2</sup> Louise Ocala,<sup>1</sup> Andrew J. Mungall,<sup>3</sup> Scott Fraser,<sup>4,5</sup> James I. McGill,<sup>6</sup> Roger A. Hitchings,<sup>4</sup> Peng T. Khaw,<sup>4</sup> Jane C. Sowden,<sup>5</sup> Sue Povey,<sup>2</sup> Michael A. Walter,<sup>7</sup> Shomi S. Bhattacharya,<sup>1</sup> and Tim Jordan<sup>1,6</sup>

**PURPOSE.** Mutations in the forkhead transcription factor gene *FOXC1* on 6p25 cause a range of ocular developmental abnormalities, with associated glaucoma. However, *FOXC1* mutations have not been found in all similarly affected pedigrees mapping to this interval. This study was undertaken to investigate the potential role of 6p25 rearrangements in causing such phenotypes.

**METHODS.** Two large families with autosomal dominant iris hypoplasia and early-onset glaucoma, 21 probands with Axenfeld-Rieger phenotypes not attributable to *PITX2* mutations, and 7 individuals with documented 6p25 cytogenetic rearrangements, were investigated by genotyping and fluorescence in situ hybridization, with markers and probes from the 6p25 region.

**RESULTS.** Interstitial 6p25 duplications were present in the unrelated families with iris hypoplasia, whereas an interstitial 6p25 deletion was identified in one Axenfeld-Rieger pedigree. Larger cytogenetic rearrangements, leading to trisomy or monosomy of the 6p25 region, resulted in microcornea and Rieger syndrome phenotypes, respectively. All the rearrangements encompassed *FOXC1*, increasing or decreasing the number of *FOXC1* copies present, and appeared to correlate with the phenotypes observed.

**CONCLUSIONS.** These findings represent the first example of both interstitial duplications and deletions cosegregating with a human developmental disorder that is attributable to altered dose of transcription factor. The data presented provide additional evidence for the pathogenicity of altered gene dosage of

*FOXC1* and suggest that a common mechanism is responsible for rearrangements of 6p25. (*Invest Ophthalmol Vis Sci.* 2002; 43:1843-1849)

Glaucoma is a heterogeneous group of disorders, characterized by chronic retinal ganglion cell loss and progressive visual damage. It represents the most common cause of irreversible blindness worldwide and is now recognized to have a major genetic basis, with six causative genes identified to date. One of these, the forkhead transcription factor gene *FOXC1* on 6p25, has been shown to be mutated in patients with a diverse spectrum of ocular developmental defects with associated glaucoma, including Axenfeld anomaly, Rieger anomaly, Rieger syndrome, and iris hypoplasia.<sup>1-3</sup> Because four such pedigrees map to 6p25 but do not contain *FOXC1* mutations and recombination events in two of them exclude *FOXC1* from the disease-causing interval,<sup>2</sup> it has been proposed that a second glaucoma-causing gene (*IRID1b* locus) lies in this region.

We have recently reported a large pedigree with a chromosomal duplication encompassing *FOXC1*, indicating that gene duplication can cause developmental disease in humans and that increased *FOXC1* gene dosage is the probable mechanism responsible for the observed iris hypoplasia and glaucoma phenotype.<sup>4</sup> Different sized duplications encompassing all three forkhead genes (*FOXC1*, *FOXF2*, and *FOXQ1*) on 6p25 and a telomeric deletion of 6p have also been described.<sup>5</sup>

In this article, we report additional families with a spectrum of 6p25 cytogenetic abnormalities, including one with an interstitial duplication and one with an interstitial deletion. The existence of interstitial duplications and deletions in the same chromosomal region implies a common cause of these cytogenetic abnormalities, that may be operating in other regions of the genome where forkhead genes are clustered. It also provides insight into developmental gene dosage as a cause of human disease.

## METHODS

### Family and Clinical Data

Two unrelated pedigrees in the United Kingdom (A and B) with identical iris hypoplasia phenotypes<sup>4,6</sup> (Figs. 1A, 1B) were studied along with individuals C through I (Fig. 2) with ocular anterior segment malformations and known 6p25 cytogenetic abnormalities. A separate panel of 21 probands with Axenfeld-Rieger phenotypes, who did not carry *PITX2* mutations, were also genotyped. Clinical assessment included slit-lamp biomicroscopy, gonioscopy, optic disc examination and anterior segment photography. The study had the approval of Moorfields Eye Hospital ethics committee and conformed to the tenets of the Declaration of Helsinki. Informed consent was obtained from all participants.

From the <sup>1</sup>Department of Molecular Genetics, Institute of Ophthalmology, London, United Kingdom; the <sup>2</sup>Department of Biology, and <sup>3</sup>Institute of Child Health, University College, London, United Kingdom; <sup>4</sup>The Sanger Centre, Wellcome Trust Genome Campus, Hinxton Hall, United Kingdom; <sup>5</sup>Moorfields Eye Hospital, London, United Kingdom; the <sup>6</sup>Eye Unit, Southampton General Hospital, Southampton, United Kingdom; and the <sup>7</sup>Departments of Ophthalmology and Medical Genetics, University of Alberta, Edmonton, Alberta, Canada.

Supported by grants from the International Glaucoma Association and Moorfields Eye Hospital Special Trustees; the Glaucoma Research Foundation; the Tadpoles Group (IGA), and the Iris Fund. Work at the Sanger Centre is funded by the Wellcome Trust. TJ was supported by Wellcome Trust Grant No. 040361-Z-94.

Submitted for publication September 26, 2001; revised January 11, 2002; accepted February 1, 2002.

Commercial relationships policy: N.

The publication costs of this article were defrayed in part by page charge payment. This article must therefore be marked "advertisement" in accordance with 18 U.S.C. §1734 solely to indicate this fact.

Corresponding author: Ordan J. Lehmann, Department of Molecular Genetics, Institute of Ophthalmology, Bath Street, London, UK EC1V 9EL; ojl@lehmman@yahoo.com.

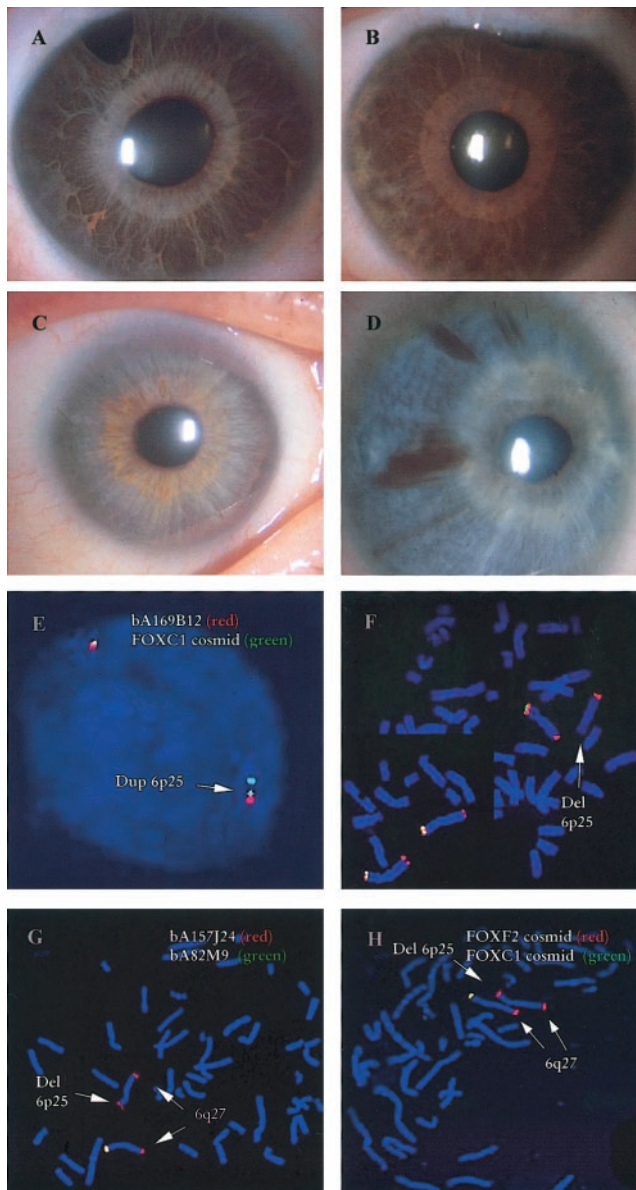


**FIGURE 1.** Ocular anterior segment photographs and FISH montages from members of the pedigrees and normal control subjects. (A) Left eye of individual from pedigree A displaying the characteristic iris hypoplasia phenotype in which iris stromal atrophy exposes the underlying iris sphincter, visible as a pale ring encircling the pupil. A surgical iridectomy is present at 11 o'clock. (B) Left eye of individual from pedigree B showing the same iris phenotype. The glistening reflex at the top of the image represents the drainage bleb from glaucoma filtration surgery. (C) Photograph (at same magnification) of individual D, showing microcornea (reduced corneal diameter). (D) Photograph showing pupillary distortion and iris anomalies (thinning) characteristic of Rieger syndrome (pedigree J). (E) Interphase nucleus preparation from individual VIII:24 (pedigree B) showing a double signal for the *FOXC1*-containing cosmid. (F) Montage of metaphase chromosome preparations from individual F (and unaffected sibling, bottom left). One chromosome 6 homologue (arrow) displays a red signal from the 6q27 control cosmid and no signal from either of the 6p25 clones bA82M9 (red) or dJ1077H22 (green), consistent with a 6p25 telomeric deletion. (G) Metaphase chromosomes from pedigree B (individual 3) showing a complete deletion of bA82M9 and a partial deletion of bA157J24. (H) Metaphase chromosomes from pedigree J (individual 3) showing deletion involving the *FOXC1*-containing, but not the *FOXF2*-containing, cosmid.

## Genotyping

Genomic DNA from pedigree B was amplified with primers for the following 6p25-localized microsatellite markers: *D6S1600*, *D6S942*, *D6S967*, *D6S344*, *D6S1713*, and *D6S1574*. The PCR products were separated by electrophoresis on 6% nondenaturing polyacrylamide gels (Protegel; National Diagnostics, Atlanta, GA), stained with ethidium bromide, and genotyped manually, as previously described.<sup>4</sup> Differences in the staining intensity of the amplified alleles were assessed visually and confirmed by densitometry (GeneTools; Synoptics, Cambridge, UK).

Chromosome preparations from individuals C through I had been analyzed in several reference laboratories, and genotyping was performed to confirm the documented cytogenetic abnormalities (using markers listed in the appendix). Individuals from the Axenfeld-Rieger cohort were initially genotyped with two markers adjacent to *FOXC1*, *D6S967*, and *AMO1* (forward, CTGGTAAGAAGGGTTGAGG; reverse, AGTTCCAATAGTCAACTTGCC, annealing temperature [ $T_a$ ] 55°C) and any found to exhibit a single allele was genotyped with additional markers (27919-73, forward, TGTGACTGCACTGGAAGAACA; reverse, AGTGTGGAGTTGCATCTTGC;  $T_a$  60°C; *FM4*, forward, TTTTG-TATTCCTTGGACCG-3', reverse, GTACGGTTTCTCCAAGGCTG,  $T_a$  57°C).

## Fluorescence In Situ Hybridization

Fluorescence in situ hybridization (FISH) involves the hybridization of labeled DNA probes to complementary sequences on chromosome preparations and detection of the hybrids with fluorescence-labeled molecules.<sup>7</sup> FISH represents a powerful technique for demonstrating the presence of a cytogenetic abnormality through comparison between the number of hybridization signals present in patients and control subjects. In the presence of a duplication, for instance, three signals are generally observed (two on one homologue and one on the other), compared with two signals in control subjects (one on each homologue). Background variation also occurs in the number of signals per cell, owing to factors that include incomplete synchronization of cultured cells within the cell cycle and viewing in two dimensions objects that are actually separated in three dimensions, which can lead to signal masking. For this reason, a large number of interphase nuclei were imaged from each individual studied.

FISH was performed on chromosome preparations obtained from short-term peripheral blood cultures or Epstein-Barr virus-transformed lymphoblastoid cell lines, from representative individuals in pedigrees A (individuals 13, 14, and 15), B (VIII:24 and IX:5), and J (individuals 2, 3, and 4); individual F; and unaffected control subjects. Probes for FISH were prepared from chromosome 6p25 clones (Table 1), plus *FOXC1*- and *FOXF2*-containing cosmids labeled with biotin or digoxigenin, either by nick translation or random priming. After hybridization to interphase nuclei or metaphase chromosomes, the probes were detected using fluorescein isothiocyanate avidin and rhodamine anti-digoxigenin, as described elsewhere.<sup>8</sup> Signals were analyzed with fluorescence microscopy, a cooled charge-coupled device (CCD; Photometrics) and FISH software (Quips; Vysis, Downers Grove, IL), enabling the number of distinct signals in each interphase nucleus to be accurately determined.

None of the interphase nuclei displayed three or more widely separated hybridization signals. Therefore, the presence of three signals was most easily interpreted as two signals on one homologue and one signal on the other (indicating a duplication), and four signals (two on each homologue) indicating a cell in G2. The proportion of nuclei with asymmetric hybridization signals, defined as two signals on one homologue and one signal on the other (or one plus a cluster of signals or two plus a cluster of signals), was recorded for subsequent statistical analysis.

## Contig Assembly and Sequence Analysis

A PAC/BAC (P1 bacteriophage-artificial chromosome/bacterial-artificial chromosome) contig spanning *FOXC1* was established using PACs

A	Interstitial Duplication	Iris Hypoplasia
B	Interstitial Duplication	Iris Hypoplasia
C	[Dup 6p22-pter]	Microcornea
D	[Dup 6p21-pter]	Microcornea
E	[Dup 6p21.2-pter]	Microcornea
F	[Del 6p25-pter]	Rieger Syndrome
G	[Del 6p24.2-pter]	Rieger Syndrome
H	[Del 6p21-pter]	Rieger Syndrome
I	[Del 6p24-pter]	Rieger Syndrome
J	Interstitial Deletion	Rieger Anomaly

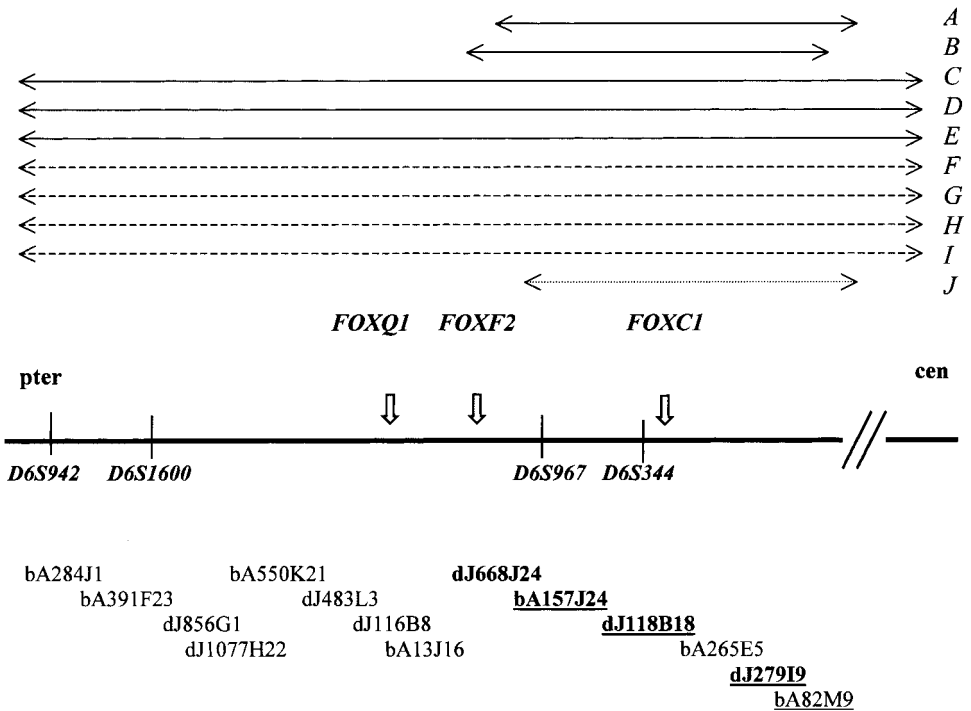


**FIGURE 2.** Physical map of the 6p25 region. The relative positions of the three forkhead genes, the extent of the duplicated or deleted (*dashed arrows*) regions in the pedigrees, and the location of the PAC/BAC clones are shown. Clones demonstrated by FISH to be duplicated (in pedigrees A and B) or deleted (pedigree J), are depicted in *bold* or *underlined typeface*. (Clone bA265E5 was not tested.) Clones prefixed bA, are from the Roswell Park BAC library and those prefixed dJ are from the RP1, -3, -4, and -5 segments of the PAC library.

isolated by screening the RPCII library with *D6S344* (dJ118B18 and dJ135A7) and also clones sequenced at the Sanger Centre. Sequence-tagged site (STS) content mapping and sequence alignment (SeqMan II and MegAlign; DNASTar, Inc., Madison, WI) confirmed the orientation of clones and relative positions of microsatellite markers (Fig. 2). Sequence analysis of selected clones was performed using NIX, a web-based suite of prediction programs. These programs, which include GRAIL, Fex, HMMgene, GENSCAN, Genemark, FGene, and BLAST for DNA analysis, with additional programs for screening sequence databases, are all available from the Human Genome Mapping Project (HGMP) Web site (see Appendix).

**RESULTS**

In light of our having previously demonstrated the presence of a duplication in pedigree A,<sup>4</sup> this study was designed to characterize the extent of the 6p25 cytogenetic abnormality present in this and other families, with the use of genotyping and FISH. Initial analysis of pedigree B, by genotyping with 6p25-localized microsatellite markers (*D6S967* and *D6S344*), yielded PCR product of increased-density ethidium bromide staining in affected compared with unaffected individuals. These qualitative findings, indicative of increased dose of PCR products, were supported by image analysis with digital quantification software (data not shown). FISH was performed to confirm these findings and demonstrated that the signal from chromosome 6p25 clones dJ668J24, bA157J24, dJ118B18,

dJ135A7, and dJ279I9 and a *FOXC1*-containing cosmid were significantly more frequently asymmetrical in affected individuals from pedigree B compared with control subjects ( $P < 0.01$ ; Table 1). Similar results were obtained from nuclei prepared from individuals in pedigree A, even though these two pedigrees were unrelated and had different haplotypes (data not shown). The signal from a *FOXF2*-containing cosmid was significantly more frequently asymmetrical in affected individuals from pedigree B than in control subjects. This was not the case in pedigree A, indicating a difference in the telomeric extent of the two duplications. NIX analysis of the clones corresponding to the interstitial duplications (A and B) demonstrates the presence of *FOXC1*, *FOXF2*, and three exons of guanosine diphosphate (GDP)-mannose 4,6-dehydratase (GMDS).

The screening of 21 Axenfeld-Rieger probands for 6p25 cytogenetic abnormalities identified one individual (J) with Rieger anomaly, monosomic for the interval *D6S967* to 279-73, a region that includes *FOXC1*, but neither *FOXF2* or *FOXQ1*. Similar genotyping results were obtained from the two other affected family members (Fig. 3) and FISH analysis of 20 metaphase chromosome spreads from each of these three affected individuals (2, 3, and 4) consistently demonstrated that the hybridization signal from clones encompassing *FOXC1*, but not *FOXF2*, was absent from one homologue (Figs. 1G, 1H, Table 1).

TABLE 1. Summary of the Proportion and Number of Cells Displaying Asymmetric Numbers of Signals on Each Homologue

	dJ483L3	FOXF2 Cosmid	dJ668J24	ba157J24	dJ118B18	FOXC1 Cosmid	dJ135A7	dJ27919	ba82M9
Pedigree A	18 (71) ( $\chi^2 = 1$ , $P = 0.46$ )	50 (101) ( $\chi^2 = 2$ , $P = 0.1$ )	43 (172) ( $\chi^2 = 10$ , $P = 0.002$ )	59 (118) ( $\chi^2 = 11$ , $P = 0.001$ )	61 (124) ( $\chi^2 = 27$ , $P < 0.001$ )	66 (156) ( $\chi^2 = 25$ , $P < 0.001$ )	55 (187) ( $\chi^2 = 13$ , $P = 0.001$ )	59 (118) ( $\chi^2 = 33$ , $P < 0.001$ )	51 (204) ( $\chi^2 = 14$ , $P < 0.001$ )
Pedigree B	20 (40) ( $\chi^2 = 2$ , $P = 0.218$ )	56 (170) ( $\chi^2 = 7$ , $P = 0.009$ )	62 (131) ( $\chi^2 = 46$ , $P < 0.001$ )	71 (141) ( $\chi^2 = 28$ , $P < 0.001$ )	62 (130) ( $\chi^2 = 29$ , $P < 0.001$ )	68 (210) ( $\chi^2 = 32$ , $P < 0.001$ )	53 (77) ( $\chi^2 = 8$ , $P = 0.004$ )	60 (119) ( $\chi^2 = 34$ , $P < 0.001$ )	39 (162) ( $\chi^2 = 0.3$ , $P = 0.6$ )
Control individual	15 (46) Present	44 (44) Present	31 (96) (Not performed)	38 (38) Partially deleted	29 (29) Deleted	36 (36) Deleted	31 (23) (Not performed)	30 (60) Deleted	37 (113) Deleted
Pedigree J metaphase FISH									

Asymmetric is defined as two signals on one homologue and one signal on the other, or one plus a cluster of signals, or two plus a cluster of signals. Statistical analysis was performed with a Yates-corrected  $\chi^2$  test. Data are percentage of cells, with the number of cells in parentheses. Underscores data, as in Figure 2.

Of the seven individuals with telomeric cytogenetic abnormalities, the three trisomic for 6p25—individual C: 46XX, dup (6p22-pter); individual D: 46XY, -7 + der (7)t (6;7) (p21;q35); and individual E: 46XY, -12 + der (12)t (6,12) (p21.2; p13.1)—exhibited the same ocular phenotype of microcornea (corneal diameter ~8.5 mm compared with the normal range of 10.6–11.75 mm), as well as ptosis. The axial lengths were normal and no iris hypoplasia was present (Fig. 1C). The four monosomic for 6p25—individual F: 46XX, del (6) (p25-pter); individual G: 46XY, -6 + der (6)t (4,6) (q33;p24.2); individual H: 46XX, del (6) (p24-pter); and individual I: 46XX, -6 + der(6)t (5,6) (q34;p24)—were diagnosed as Rieger syndrome. All had combinations of anterior segment developmental defects, dental abnormalities, varying degrees of hearing impairment, and developmental delay, without the umbilical abnormalities characteristically associated with this condition. Brain imaging had been conducted in only one individual (I), revealing hydrocephalus.

## DISCUSSION

An increasing body of evidence, derived from a range of species, indicates that altered dose of *FOXC1* causes a spectrum of developmental phenotypes with examples including the dose-dependent role of *Foxc1* in cardiovascular, renal, somite, and ocular development.<sup>9–13</sup> The latter is illustrated by the naturally occurring *Foxc1* mutant which in the homozygous state results in the congenital hydrocephalus (*cb*) phenotype, which has more severe ocular (and nonocular) developmental anomalies than do *cb* heterozygotes.<sup>14,15</sup> Such murine phenotypes resemble those present in patients with mutations or deletions involving *FOXC1*.

All previous reports of 6p25 cytogenetic abnormalities<sup>4,5,16</sup> are consistent with the concept that altered dose of a gene or genes in the duplicated or deleted region results in the ocular developmental phenotype(s) observed. Although *FOXC1* is the most likely candidate because of its known role in anterior segment development, the presence of adjacent forkhead genes and mapping data for the *IRID1b* locus<sup>2</sup> have prevented the exclusion of alternative hypotheses. The demonstration of a duplication in a pedigree (B) in which a single recombination event appeared to exclude *FOXC1* from the disease-causing interval, removes one of the two defining recombinants for the *IRID1b* locus.<sup>2</sup> Difficulty interpreting the original linkage data, stemmed from the method of visualizing alleles (<sup>32</sup>P), which did not allow differences in the dose of identical-sized alleles to be easily resolved. The recombinant individual VIII:24, despite having a crossover with *D6S344*, has inherited a third copy of *FOXC1*, like all other affected individuals in pedigree B (Fig. 1E). This situation is reminiscent of the mapping of Charcot-Marie-Tooth disease, which was also complicated by an unrecognized duplication.<sup>17,18</sup>

Confirmation that increased dose of *FOXC1* is pathogenic requires recapitulation of the human phenotype in an animal model carrying an additional functional copy of *FOXC1*, a goal we are currently working toward. In the interim the observation of multiple *FOXC1*-containing interstitial cytogenetic rearrangements, which in two pedigrees (A and J) did not include other forkhead genes, coupled with data on *Foxc1* from other species and the weakened case for *IRID1b*, suggest but do not prove, that altered dose of *FOXC1* is pathogenic. Because early-onset glaucoma will develop in almost all the affected individuals in the duplication pedigrees (A and B),<sup>4,6</sup> it appears that interstitial duplication results in a higher rate of glaucoma than either deletion or *FOXC1* mutation (~50% of cases).<sup>19</sup>

In the small series of telomeric cytogenetic abnormalities presented in this article, the telomeric deletions result in

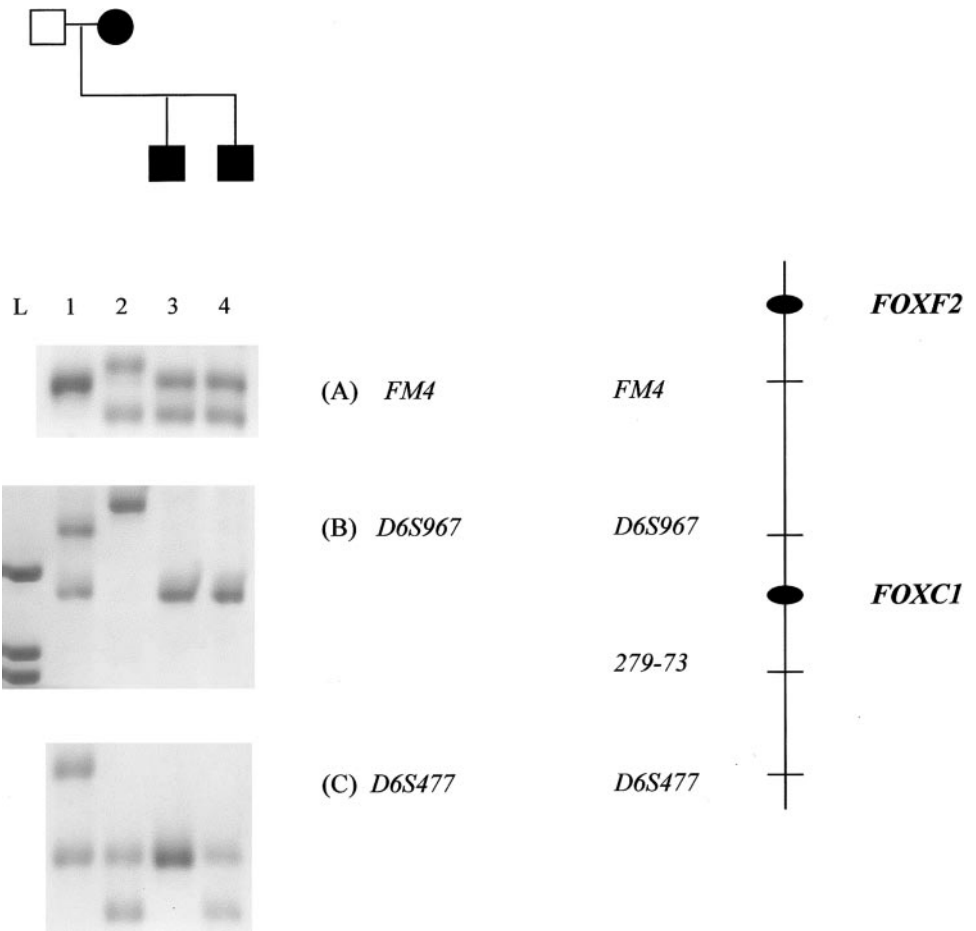


**FIGURE 3.** Genotyping results showing evidence of an interstitial deletion in pedigree J. Montage of photographs of ethidium bromide-stained gel showing PCR products for selected 6p25 microsatellite markers (A) *FM4*, (B) *D6S967*, and (C) *D6S477*. Lanes 2, 3, and 4: affected individuals (filled symbols) were monosomic for *D6S967* but not for *FM4* or *D6S477*, indicating that the interstitial deletion did not involve *FOXF2*.

Rieger syndrome, the severest phenotype in the Axenfeld-Rieger spectrum. One of these deletions was associated with hydrocephalus and is in keeping with previous reports.<sup>14</sup> Large telomeric duplications were associated with a microcornea phenotype (individuals C-E) in contrast to the iris hypoplasia phenotype, with the much smaller interstitial duplications (A and B), supporting a correlation between the phenotype and the extent of the cytogenetic abnormality. It also raises the intriguing possibility that the balance between the dose of gene, or genes, in the smaller (interstitial) and larger (telomeric) duplicated segments influences the dimensions of the ocular anterior segment. One candidate for such an interaction, known to be expressed in the eye, is the transcription factor gene *TFAP2α*, which lies within the region duplicated in individuals C through E.<sup>20</sup>

The identification of multiple interstitial cytogenetic abnormalities on 6p25 has interesting implications for the mechanisms underlying chromosomal rearrangements. These rearrangements are associated with a wide variety of genetic disorders and most frequently arise from homologous recombination between low-copy-number repetitive sequences. Interstitial duplications and deletions coexist in only a handful of disorders such as Charcot-Marie-Tooth disease (CMT/hereditary neuropathy with liability to pressure palsies [HNPP]), Smith Magenis syndrome (SMS), red-green color blindness, thalassemia, and derivative 22 syndrome/velo-cardio-facial/Di-George syndrome.<sup>21,22</sup> In two examples (CMT/HNPP and SMS) the flanking sequences responsible for these contiguous gene duplication-deletion syndromes have been characterized.<sup>23-25</sup> The demonstration of duplications in unrelated iris hypoplasia pedigrees led us to predict the existence of a similar mecha-

nism, from which cases of other 6p25 cytogenetic abnormalities would be expected to arise. A panel of probands with anterior segment malformations was screened to test this hypothesis. The identification of a pedigree (J) with an interstitial deletion indicates that the 6p25 region is susceptible to chromosomal rearrangements.

Although the cause of these rearrangements is currently unknown, two mechanisms can be postulated. The first, homologous recombination and unequal crossing over, is dependent on the presence of significant regions of sequence homology.<sup>26</sup> Although homologous sequence exists on 6p25, including the three forkhead genes (*FOXC1*, *FOXF2*, and *FOXQ1*), which share 70% to 75% sequence identity across their conserved forkhead domains, the variable extent of the duplication in these and other families<sup>5</sup> argues against such a hypothesis. Alternatively, a novel, as yet unknown mechanism could be responsible, such as that which occurs in the rare X-linked condition, Pelizaeus-Merzbacher disease, in which duplications and deletions of differing size cause central nervous system (CNS) demyelination through altered dose of the proteolipid protein gene.<sup>27,28</sup> Whatever the mechanism, it may be relevant to other areas of the genome, especially those containing forkhead gene clusters (e.g., 1p32, 12p13, 14q13, and 17q25). One such cluster, *FOXC2/FOXF1/FOXLI*, on 16q24 is relevant to ocular development, because it lies within the critical interval for a Rieger syndrome locus<sup>29</sup> and haploinsufficiency of *Foxc2* (and *Foxc1*) causes ocular anterior segment anomalies in mice.<sup>30</sup> In view of the similarity to the 6p25 forkhead cluster (*FOXC1/FOXF2/FOXQ1*), it will be interesting to determine whether cytogenetic rearrangements underlie the 16q24-linked Axenfeld-Rieger phenotype.

The pedigrees with interstitial duplications and deletions reported in this article provide evidence for a common mechanism, causing cytogenetic rearrangements and a range of ocular developmental defects. The presence of 6p25 interstitial duplications and deletions represents the first example of both types of cytogenetic abnormalities causing a human developmental phenotype through presumed altered gene dosage of transcription factor. These findings add to the limited number of disorders in which pairs of interstitial duplications and deletions have been described and suggest that other cytogenetic abnormalities, such as inversions or hybrid genes, may be found in this region. It remains to be determined whether the pathogenicity of altered gene dosage, suggested with *FOXC1* and previously demonstrated with *PAX6*,<sup>31</sup> applies more generally to transcription factors.

### Acknowledgments

The authors thank the members of the families for their help with this study and Beverly Searle for use of the *Unique* offline database (www.rarechromo.org) to identify suitable research subjects; Andrew Webster for the use of his contiguous repeat sequence detector program; Yvonne Edwards for the 6q27 cosmid; Glen Brice and Anne Child for assisting with the provision of a blood sample from individual J; especially, all members of the Chromosome 6 Project Group at the Sanger Centre for mapping and sequencing data; and the Medical Research Council's Human Gene Mapping Program (HGMP) Resource Centre for the provision of the probes and the NIX analysis program.

### References

- Nishimura D, Swiderski R, Alward W, et al. The forkhead transcription factor gene FKHL7 is responsible for glaucoma phenotypes which map to 6p25. *Nat Genet.* 1998;19:140-147.
- Mears AJ, Jordan T, Mirzayans F, et al. Mutations of the forkhead/winged-helix gene, FKHL7, in patients with Axenfeld-Rieger anomaly. *Am J Hum Genet.* 1998;63:1316-1328.
- Mirzayans F, Gould DB, Heon E, et al. Axenfeld-Rieger syndrome resulting from mutation of the FKHL7 gene on chromosome 6p25. *Eur J Hum Genet.* 2000;8:71-74.
- Lehmann OJ, Ebenezer ND, Jordan T, et al. Chromosomal duplication involving the forkhead transcription factor gene FOXC1 causes iris hypoplasia and glaucoma. *Am J Hum Genet.* 2000;67:1129-1135.
- Nishimura DY, Searby CC, Alward WL, et al. A spectrum of FOXC1 mutations suggests gene dosage as a mechanism for developmental defects of the anterior chamber of the eye. *Am J Hum Genet.* 2001;68:364-372.
- Jordan T, Ebenezer N, Manners R, McGill J, Bhattacharya S. Familial iridogoniodysplasia maps to a 6p25 region implicated in primary congenital glaucoma and iridogoniodysgenesis anomaly. *Am J Hum Genet.* 1997;61:882-888.
- Ekong R, Wolfe J. Advances in fluorescent in situ hybridisation. *Curr Opin Biotechnol.* 1998;9:19-24.
- Fox M, Povey S. Fluorescent in situ hybridization (FISH) to mouse chromosomes. In: Jackson IJ, Abbott CM, eds. *Mouse Genetics and Transgenics: A Practical Approach*. New York: Oxford University Press; 2000:154-169.
- Kidson SH, Kume T, Deng K, Winfrey V, Hogan BL. The forkhead/winged-helix gene, Mf1, is necessary for the normal development of the cornea and formation of the anterior chamber in the mouse eye. *Dev Biol.* 1999;211:306-322.
- Topczewska JM, Topczewski J, Solnica-Krezel L, Hogan BL. Sequence and expression of zebrafish *foxc1a* and *foxc1b*, encoding conserved forkhead/winged helix transcription factors. *Mech Dev.* 2001;100:343-347.
- Winnier GE, Kume T, Deng K, et al. Roles for the winged helix transcription factors Mf1 and Mfb1 in cardiovascular development revealed by nonallelic noncomplementation of null alleles. *Dev Biol.* 1999;213:418-431.
- Kume T, Deng K, Hogan BL. Murine forkhead/winged helix genes Foxc1 (Mf1) and Foxc2 (Mfb1) are required for the early organogenesis of the kidney and urinary tract. *Development.* 2000;127:1387-1395.
- Kume T, Jiang H, Topczewska JM, Hogan BL. The murine winged helix transcription factors, Foxc1 and Foxc2, are both required for cardiovascular development and somatogenesis. *Gen Dev.* 2001;15:2470-2482.
- Kume T, Deng K, Winfrey V, Gould DB, Walter MA, Hogan BL. The forkhead/winged helix gene Mf1 is disrupted in the pleiotropic mouse mutation congenital hydrocephalus. *Cell.* 1998;93:985-996.
- Hong H, Lass JH, Chakravarti A. Pleiotropic skeletal and ocular phenotypes of the mouse mutation congenital hydrocephalus (*cb/Mf1*) arise from a winged helix/forkhead transcription factor gene. *Hum Mol Genet.* 1999;8:625-637.
- Law CJ, Fisher AM, Temple IK. Distal 6p deletion syndrome: a report of a case with anterior chamber eye anomaly and review of published reports. *J Med Genet.* 1998;35:685-689.
- Lupski JR, de Oca-Luna RM, Slaugenhaupt S, et al. DNA duplication associated with Charcot-Marie-Tooth Disease Type 1A. *Cell.* 1991;66:219-232.
- Matise TC, Chakravarti A, Patel PI, et al. Detection of tandem duplications and implications for linkage analysis. *Am J Hum Genet.* 1994;54:1110-1121.
- Walter MA, Kulak KC, Héon E, et al. Comparison of genotype with glaucoma incidence and treatment in Axenfeld-Rieger patients [ARVO Abstract]. *Invest Ophthalmol Vis Sci.* 2000;41(4):S527. Abstract nr 2809.
- Davies A, Mirza G, Flinter F, Ragoussis J. An interstitial deletion of 6p24-p25 proximal to the FKHL7 locus and including AP-2 $\alpha$  that affects anterior eye chamber development. *J Med Genet.* 1999;36:708-710.
- Lupski JR. Genomic disorders: structural features of the genome can lead to DNA rearrangements and human disease traits. *Trends Genet.* 1998;14:417-422.
- Edelmann L, Pandita RK, Spiteri E, et al. A common molecular basis for rearrangement disorders on chromosome 22q11. *Hum Mol Genet.* 1999;8:1157-1167.
- Reiter LT, Murakami T, Koeuth T, et al. A recombination hotspot responsible for two inherited peripheral neuropathies is located near a mariner transposon-like element. *Nat Genet.* 1996;12:288-297.
- Chen KS, Manian P, Koeuth T, et al. Homologous recombination of a flanking repeat gene cluster is a mechanism for a common contiguous gene deletion syndrome. *Nat Genet.* 1997;17:154-163.
- Potocki L, Chen KS, Park SS, et al. Molecular mechanism for duplication 17p11.2: the homologous recombination reciprocal of the Smith-Magenis microdeletion. *Nat Genet.* 2000;24:84-87.
- Waldman AS, Liskay RM. Dependence of intrachromosomal recombination in mammalian cells on uninterrupted homology. *Mol Cell Biol.* 1988;8:5350-5357.
- Woodward K, Kendall E, Vetrie D, Malcolm S. Pelizaeus-Merzbacher disease: identification of Xq22 proteolipid-protein duplications and characterisation of breakpoints by interphase FISH. *Am J Hum Genet.* 1998;63:207-217.
- Woodward K, Malcolm S. Proteolipid protein gene: Pelizaeus-Merzbacher disease in humans and neurodegeneration in mice. *Trends in Genetics.* 1999;15:125-128.
- Nishimura DY, Searby CC, Borges AS, et al. Identification of a fourth Rieger Syndrome locus on 16q24. *Am J Hum Genet.* 2000;67:S2146:383.
- Smith RS, Zabaleta A, Kume T, et al. Haploinsufficiency of the transcription factors FOXC1 and FOXC2 results in aberrant ocular development. *Hum Mol Genet.* 2000;9:1021-1032.
- Schedl A, Ross A, Lee M, et al. Influence of PAX6 gene dosage on development: over expression causes severe eye abnormalities. *Cell* 1996;86:71-82.

**APPENDIX****Genotyping Markers**

Individuals C through I were genotyped with the following markers: *D6S1617*, *D6S1640*, *D6S1598*, *D6S1547*, *D6S1674*, *D6S296*, *D6S410*, *D6S470*, *D6S1653*, *D6S263*, *D6S1600*, *D6S942*, *D6S967*, *D6S344*, *D6S1713*, and *D6S1574*, all amplified according to the manufacturer's (Research Genetics, Huntsville, AL) recommended conditions.

**Electronic Database Information and Accession Numbers**

NIX is provided by the Medical Research Council's Human Genome Mapping Project Resources Centre (Cambridge, UK) and is available at <http://www.hgmp.mrc.ac.uk/gdb-bin/>.

Online Mendelian Inheritance in Man (OMIM), is provided by the National Center for Biotechnology Information, National Institutes of Health (Bethesda, MD) and is available at <http://www.ncbi.nlm.nih.gov/omim/>. Gene accession numbers: *PITX2* (OMIM 601542), *FOXC1* (601090), *FOXC2* (602402), *FOXF1* (601089), *FOXF2* (603250), *FOXL1* (603252), *TFAP2 $\alpha$*  (107580), and *GMD5* (602884).

Chromosome 6 Project, Sanger Centre (Hinxton Hall, UK), available at <http://www.sanger.ac.uk/HGP/Chr6/>. Clone accession numbers: bA284J1 (AL392183), bA391F23 (AL356130), dJ856G1 (AL033381), dJ1077H22 (AL133402), bA550k21 (AL353618), dJ483L3 (AL035531), dJ116B8 (AL589989), bA13J16 (AL499606), dJ668J24 (AL034346), bA157J24 (AL512329), dJ118B18 (AL034344), bA265E5 (AL451141), dJ279I9 (AL033517), and bA82M9 (AL137179).